Controllability Analysis of an Ethanol Water Distillation Coloumn

Willem Adriaan Smit
14052131

CBT

2019-04-28

Controllability Analysis of an Ethanol Water Distillation Coloumn

Willem Adriaan Smit

14052131

Department of Chemical Engineering
University of Pretoria

CBT

2019-04-28

Controllability Analysis of an Ethanol Water Distillation Coloumn

Synopsis

Welcome to the Noob's guide. This section has only been included for reference on how to use it when comparing the source code to the resulting document. Please continue to the Introduction, Section **??**.

Contents

Synopysis **iii**

1 Introduction **1**

2 Process Model Description **2**

2.1 System Diagram 2

2.2 System Description 2

2.3 Measurement of Variables 3

2.4 System Variables 3

2.5 System Model 4

2.6 Scaling the System 5

3 Controllability Analysis **7**

3.1 Minimal Realisation of the System 8

3.2 Functional Controllability 8

3.3 System Poles 9

3.3.1 Calculating the System Poles 9

3.3.2 Calculating the System Pole Directions 10

3.3.3 Discussion of System Poles 10

3.4 System Zeros 10

3.4.1 Calculating the System Zeros 10

3.4.2 Calculating the System Zero Directions 11

3.4.3 Discussion of System Zeros 13

List of Figures

1 Vapour Liquid Equilibrium (VLE) data for the water ethanol system at 1 bar. 1

2 Process flow diagram of the system 2

3 Overhead composition response to a pulse of 15 minutes duration in the reflux rate. 5

4 Side stream composition response to a pulse of 15 minutes duration in feed temperature. 5

5 The singular values of $G(j\omega)$. 9

6 A graphical representation of the system's poles and zeros. 13

List of Tables

1 Summary of all the model variables. 4

2 The boundaries of the manipulated variables in the system. 6

3 The boundaries of the controlled variables in the system. 6

4 The boundaries of the controlled variables in the system. 6

5 The poles of the system. 9

6 The pole directions of the system. 10

7 The zeros of the system. 11

8 The zero directions of the system. 12

1 Introduction

Renewable energy is becoming a major role player in the world today. As people are starting to shift away from fossil fuel based technology and energy generation, the focus is shifting to alternative methods of energy (and fuel) production.

One such a method involves the use of ethanol as an alternative fuel. Ethanol particularly is an excellent contender for a major alternative fuel, as it can be produced from crops or by means of biological fermentation. [A lot of] research is currently done on methods to generate ethanol in order for it to power the future.

Producing ethanol, however, is not the only problem to overcome. After the production process (usually from fermentation), the ethanol has to be separated from the product mixture in order to purify it. This poses to be a challenge (and a very energy intensive operation) due to the thermodynamic properties of the homogeneous mixture between water and ethanol. As noted in Figure 1, the system contains an azeotrope. This leads to very expensive separation operations, as pressure swing distillation has to be implemented for high purity separation.

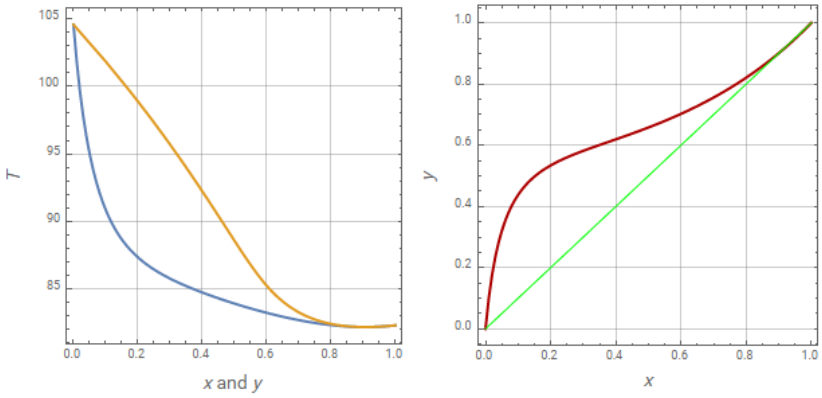

Figure 1: Vapour Liquid Equilibrium (VLE) data for the water ethanol system at 1 bar.

In this report, an investigation regarding the controllability of the ethanol water separation process is investigated. The plant investigated is a pilot plant that is testing the feasibility for scale up of the process. Control has to implemented to ensure that the system reaches a steady state, as well as to improve the overall profitability by reducing the standard deviation in the product quality.

A plant wide control system will not be investigated. Only the distillation coloumn is analysed. The current proposed control system is discussed in Section [REF!!!]. This report will investigate the validity of such a proposed control scheme, as well as the where the physical constrains in the system lies.

2 Process Model Description

2.1 System Diagram

The Process Flow Diagram of the system, with all the relevant inputs, outputs and disturbances are displayed in Figure 2.

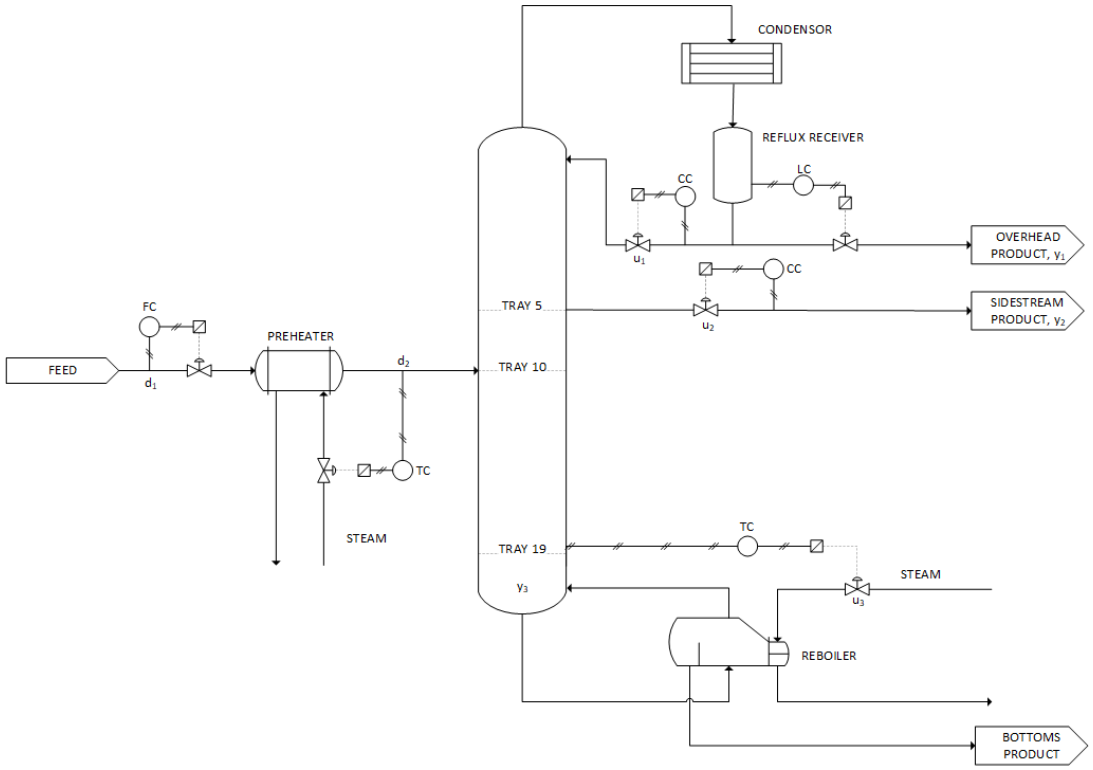

Figure 2: Process flow diagram of the system

2.2 System Description

The system involves the separation of water and ethanol (in a solution), with the aim of producing an ethanol product that can be used as an alternative fuel source.

The system can be summarized as follows:

- The distillation column of the pilot scale plant is a 19 tray, 12 inch diameter column.
- The column has variable feed and side stream draw off locations.
- The side stream flow is varied to control the composition of the stream.

- The distillate vapour draw off stream is fully condensed, and then separated into the reflux and product streams.
- The product stream is set to control the level in the condenser, while the reflux stream controls the composition of the distillate product.
- A kettle re-boiler is used to add energy to the column. Stream is the main utility.
- The amount re-boiled bottoms product is controlled by varying the steam supplied to the re-boiler.
- The feed temperature and flow rate can be controlled to simulate disturbances on the system. These variables are strictly defined as disturbances, as they are part of another section's (the bio-reactor or chemostat) control scheme.
- Currently all variables are controlled with single input single output (SISO) control loops.

2.3 Measurement of Variables

The compositions are measured/determined through various on-line sensors (densitrometry and refractometry). Temperatures are monitored using thermocouples. Flow rates are measured with thermal mass flow meters. Levels are measured by inference from static head, measured with a pressure sensor. The product model and serial numbers are not available.

2.4 System Variables

All variables in the ethanol water distillation coloumn system is summarised in Table 1. The current steady state values hold reference to the tested conditions on site.

Table 1: Summary of all the model variables.

Input Variables			
Variable	Description	Steady State Value	Units
u_1	Reflux flow rate	0.18	gpm
u_2	Side stream product flow rate	0.046	gpm
u_3	Reboiler steam pressure	20	psi
Output Variables			
Variable	Description	Steady State Value	Units
y_1	Overhead ethanol mole fraction	0.7	-
y_2	Side stream ethanol mole fraction	0.52	-
y_3	Tray #19 temperature	92	°C
Disturbance Variables			
Variable	Description	Steady State Value	Units
d_1	Feed flow rate	0.8	gpm
d_2	Feed temperature	78	°C

2.5 System Model

The model was determined by conducting pulse testing on the system. In most cases a first order plus dead time model gave a sufficiently accurate fit to experimental data. The sum of squares of an adequate fit during model development was a values of greater than 0.98. In some relationships more complex dynamics had to be derived and a second order system with a first order lag and dead time, was used to accurately describe the impulse response (based on the same adequate fit method described above). The equations used for fitting were

$$\frac{y_i(s)}{u_i(s)} = \frac{K_i e^{-\theta_i s}}{\tau_i s + 1} \tag{1}$$

for the first order plus dead time system, and

$$\frac{y_i(s)}{u_i(s)} = \frac{K_i(\tau_{1i} s + 1)e^{-\theta_i s+1}}{(\tau_{2i} s + 1)(\tau_{3i} s + 1)} \tag{2}$$

for the relationships with more complex dynamics.

The fitting curves of two pulse tests are displayed in Figure 3 and Figure 4. An important

thing to note is that the unit of time is minutes, an therefore all responses and analysis will be conducted with this unit for time.

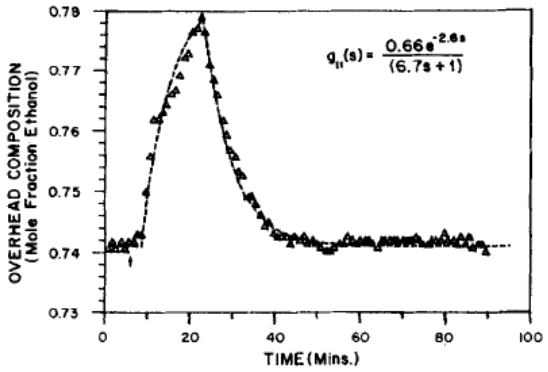

Figure 3: Overhead composition response to a pulse of 15 minutes duration in the reflux rate.

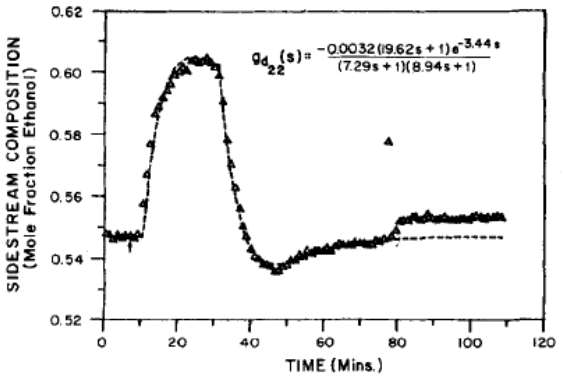

Figure 4: Side stream composition response to a pulse of 15 minutes duration in feed temperature.

The model was then written in the standard form of a linear MIMO system [REF!!!],

$$\mathbf{y}(s) = \mathbf{G}(s)\mathbf{u}(s) + \mathbf{G}_d(s)\mathbf{d}(s) \tag{3}$$

where

$$\hat{G}(s) = \begin{bmatrix} G_{11} & G_{12} & G_{13} \\ G_{21} & G_{22} & G_{23} \\ G_{31} & G_{32} & G_{33} \end{bmatrix} = \begin{bmatrix} \frac{0.66e^{-2.6s}}{6.7s+1} & \frac{-0.61e^{-3.5s}}{8.64s+1} & \frac{-0.0049e^{-s}}{9.06s+1} \\ \frac{1.11e^{-6.5s}}{3.25s+1} & \frac{-2.36e^{-3s}}{5.0s+1} & \frac{-0.012e^{-1.2s}}{7.09s+1} \\ \frac{-34.68e^{-9.2s}}{8.15s+1} & \frac{46.2e^{-9.4s}}{10.9s+1} & \frac{0.87(11.61s+1)e^{-s}}{(3.89s+1)(18.8s+1)} \end{bmatrix} \tag{4}$$

and

$$\hat{G}_d(s) = \begin{bmatrix} G_{d11} & G_{d12} \\ G_{d21} & G_{d22} \\ G_{d31} & G_{d32} \end{bmatrix} = \begin{bmatrix} \frac{0.14e^{-12s}}{6.2s+1} & \frac{-0.0011(26.32s+1)e^{-2.66s}}{(7.85s+1)(4.63s+1)} \\ \frac{0.53e^{-10.5s}}{6.9s+1} & \frac{-0.0032(19.62s+1)e^{-3.44s}}{(7.29s+1)(8.94s+1)} \\ \frac{-11.54e^{-0.6s}}{7.01s+1} & \frac{0.32e^{-2.6s}}{7.76s+1} \end{bmatrix} \tag{5}$$

2.6 Scaling the System

In order to perform a controllability analysis on the system, the system had to be scaled according to the method described in [Reff!!!].

In order to perform the scaling operation, the upper and lower limits of all the variables have to be defined. The initial boundary values of all system variables are summarized in Table 2, Table 3, and Table 4.

Table 2: The boundaries of the manipulated variables in the system.

Manipulated Variable	**Lower Constraint**	**Upper Constraint**	**Steady State Value**
u_1, Reflux Flow Rate	0.068	0.245	0.18
u_2, Side Stream Flow Rate	0.00694	0.1	0.046
u_3, Reboiler Steam Pressure	15.6	34	20

Table 3: The boundaries of the controlled variables in the system.

Controlled Variable	**Maximum Set Point Change**	**Steady State Value**
y_1, Overhead Mole Fraction Ethanol	0.05	0.7
y_2, Side Stream Mole Fraction Ethanol	0.1	0.52
y_3, Temperature on Tray #19	8	92

Table 4: The boundaries of the controlled variables in the system.

Disturbance Variable	**Lower Constraint**	**Upper Constraint**	**Steady State Value**
d1, Feed Flow Rate	0.6	1.1	0.8
d2, Feed Temperature	50	102	78

Using the information above the following matrices can be deduced, that will be used to scale the system

$$D_e = \begin{bmatrix} 0.01 & 0 & 0 \\ 0 & 0.01 & 0 \\ 0 & 0 & 4 \end{bmatrix} \tag{6}$$

$$D_u = \begin{bmatrix} 0.065 & 0 & 0 \\ 0 & 0.03906 & 0 \\ 0 & 0 & 4.4 \end{bmatrix} \tag{7}$$

$$D_d = \begin{bmatrix} 0.3 & 0 \\ 0 & 28 \end{bmatrix} \tag{8}$$

$$r = \begin{bmatrix} 0.05 & 0 & 0 \\ 0 & 0.1 & 0 \\ 0 & 0 & 8 \end{bmatrix} \tag{9}$$

Using the above matrices, the scaled system can be calculated using the following equations from [REF!!!],

$$G = D_e^{-1} \hat{G} D_u \tag{10}$$

$$G_d = D_e^{-1} \hat{G}_d D_d \tag{11}$$

From Equation 10 and Equation 11, the scaled system can be written as

$$G(s) = \begin{bmatrix} G_{11} & G_{12} & G_{13} \\ G_{21} & G_{22} & G_{23} \\ G_{31} & G_{32} & G_{33} \end{bmatrix} = \begin{bmatrix} \frac{4.29e^{-2.6s}}{6.7s+1} & \frac{-2.38266e^{-3.5s}}{8.64s+1} & \frac{-2.156e^{-s}}{9.06s+1} \\ \frac{7.215e^{-6.5s}}{3.25s+1} & \frac{-9.21816e^{-3s}}{5.0s+1} & \frac{-2.156e^{-1.2s}}{7.09s+1} \\ \frac{-0.56355e^{-9.2s}}{8.15s+1} & \frac{0.451143e^{-9.4s}}{10.9s+1} & \frac{1.1(10.1007s+0.87)e^{-s}}{(3.89s+1)(18.8s+1)} \end{bmatrix} \tag{12}$$

and

$$G_d(s) = \begin{bmatrix} G_{d11} & G_{d12} \\ G_{d21} & G_{d22} \\ G_{d31} & G_{d32} \end{bmatrix} = \begin{bmatrix} \frac{4.2e^{-12s}}{6.2s+1} & \frac{-2800(0.028952s+0.0011)e^{-2.66s}}{(7.85s+1)(4.63s+1)} \\ \frac{15.9e^{-10.5s}}{6.9s+1} & \frac{-2800(-0.062784s+0.0032)e^{-3.44s}}{(7.29s+1)(8.94s+1)} \\ \frac{-0.8655e^{-0.6s}}{7.01s+1} & \frac{2.24e^{-2.6s}}{7.76s+1} \end{bmatrix} \tag{13}$$

with

$$R = \begin{bmatrix} 5 & 0 & 0 \\ 0 & 10 & 0 \\ 0 & 0 & 2 \end{bmatrix} \tag{14}$$

3 Controllability Analysis

A full controllability analysis was performed on the system to establish whether:

1. The system has adequate set point tracking characteristics.
2. The system has adequate disturbance rejection characteristics.

The method used is described in [REF!!].

3.1 Minimal Realisation of the System

The system written in the transfer function notation is in no danger of not being a minimal realizable system. It is only when the system is converted to state space notation it runs the risk of not being a minimal realization.

When converting the transfer function model to a state space realisation of the system, it has to be noted that all dead time that is inherent to the system is ignored, as state space realizations cannot deal with dead time. The system was however converted to its state space realization, in order to cross check the calculated poles and zeros of the system.

The minimum state space realization of the system is given below.

3.2 Functional Controllability

The system has to be checked for functional controllability. This implies that outputs should be able to be controlled independently. There are two factors that have to be considered when checking for functional controllability of a system, namely

1. There have to be at least as many inputs as there are outputs
2. The rank of G(s) should be greater than the number of outputs.

For consideration 1, mentioned above, the number of inputs and outputs in the system is equal. This criteria is therefore satisfied by the system.

For consideration 2, the minimum singular value (or $\underline{\sigma}$) of $G(j\omega)$ should be non-zero. In order to determine whether the system satisfies this criteria, all the singular values, of all the outputs were computed of a wide frequency range. A bode diagram displaying the result can be seem in Figure 5.

As is clear from Figure 5, $\underline{\omega}$ never reaches zero, although it does approach zero as the frequency goes to infinity.

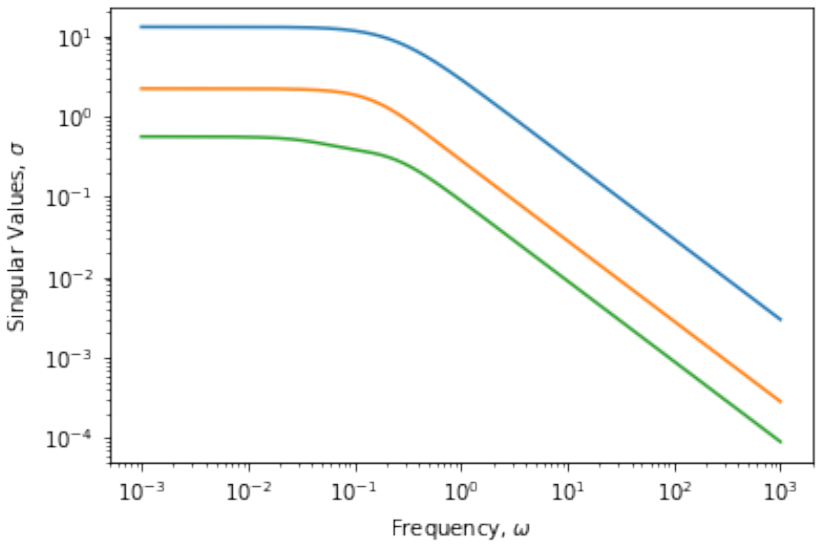

Figure 5: The singular values of $G(j\omega)$.

Based on the above information, is can be concluded that the system is indeed functional controllable. This means that the system's rank is equal to the amount of outputs that the system has.

The current selected inputs and outputs can therefore be controlled with adequate independence.

3.3 System Poles

3.3.1 Calculating the System Poles

The poles of the system was calculated. The system has a total number of six poles. The poles calculated are described in the Table 5.

Table 5: The poles of the system.

Pole	Real Part	Imaginary Part
p_1	-0.3923	0
p_2	-0.1397	0
p_3	-0.0791	0.0349
p_4	-0.0791	-0.0349
p_5	-0.0960	0.0042
p_6	-0.0960	-0.0042

3.3.2 Calculating the System Pole Directions

The pole directions of the system was calculated by substituting all the pole values into $G(s)$ and calculating the input and output directions of the relevant poles. The calculated pole direction are given Table 6.

Table 6: The pole directions of the system.

Pole	Input Direction (V)	Output Direction (U)
p_1	$\begin{bmatrix} 0.34 \\ 0.94 \\ -0.04 \end{bmatrix}$	$\begin{bmatrix} 0.80 \\ -0.07 \\ 0.60 \end{bmatrix}$
p_2	$\begin{bmatrix} -0.15 \\ 0.19 \\ 0.97 \end{bmatrix}$	$\begin{bmatrix} -0.05 \\ -0.05 \\ 1.00 \end{bmatrix}$
p_3	$\begin{bmatrix} -0.59 \\ -0.12 - 0.13j \\ -0.76 - 0.02j \end{bmatrix}$	$\begin{bmatrix} -0.11 - 0.07j \\ 0.03 - 0.03j \\ -0.78 - 0.61j \end{bmatrix}$
p_4	$\begin{bmatrix} -0.59 \\ -0.12 + 0.13j \\ -0.76 + 0.02j \end{bmatrix}$	$\begin{bmatrix} -0.11 + 0.07j \\ 0.03 + 0.03j \\ -0.78 + 0.61j \end{bmatrix}$
p_5	$\begin{bmatrix} -0.71 \\ 0.14 - 0.19j \\ -0.66 + 0.04j \end{bmatrix}$	$\begin{bmatrix} -0.31 + 0.56j \\ 0.31 + 0.55j \\ -0.09 - 0.43j \end{bmatrix}$
p_6	$\begin{bmatrix} -0.71 \\ 0.14 + 0.19j \\ -0.66 - 0.04j \end{bmatrix}$	$\begin{bmatrix} -0.31 - 0.56j \\ 0.31 - 0.55j \\ -0.09 + 0.43j \end{bmatrix}$

3.3.3 Discussion of System Poles

3.4 System Zeros

3.4.1 Calculating the System Zeros

The system zeros were calculated. The system contains a total number of nine zeros, all of them located in the left hand plane (LHP). The system zeros are given in Table 7.

Table 7: The zeros of the system.

Zero	Real Part	Imaginary Part
z_1	-0.3077	0
z_2	-0.2571	0
z_3	-0.2	0
z_4	-0.1493	0
z_5	-0.1227	0
z_6	-0.1157	0
z_7	-0.1104	0
z_8	-0.0917	0
z_9	-0.0532	0

3.4.2 Calculating the System Zero Directions

The zero directions of the system was calculated by substituting all the zero values into $G(s)$ and calculating the input and output directions of the relevant zeros using the singular value decomposition of $G(z_i)$. The calculated zero directions are given Table 8.

Table 8: The zero directions of the system.

Zero	**Input Direction** (V)	**Output Direction** (U)
z_1	$\begin{bmatrix} 1 \\ 0 \\ 0 \end{bmatrix}$	$\begin{bmatrix} 0 \\ 1 \\ 0 \end{bmatrix}$
z_2	$\begin{bmatrix} 0 \\ 0 \\ 1 \end{bmatrix}$	$\begin{bmatrix} 0 \\ 0 \\ 1 \end{bmatrix}$
z_3	$\begin{bmatrix} 0 \\ -1 \\ 0 \end{bmatrix}$	$\begin{bmatrix} 0 \\ 1 \\ 0 \end{bmatrix}$
z_4	$\begin{bmatrix} -1 \\ 0 \\ 0 \end{bmatrix}$	$\begin{bmatrix} -1 \\ 0 \\ 0 \end{bmatrix}$
z_5	$\begin{bmatrix} -1 \\ 0 \\ 0 \end{bmatrix}$	$\begin{bmatrix} 0 \\ 0 \\ 1 \end{bmatrix}$
z_6	$\begin{bmatrix} 0 \\ 1 \\ 0 \end{bmatrix}$	$\begin{bmatrix} -1 \\ 0 \\ 0 \end{bmatrix}$
z_7	$\begin{bmatrix} 0 \\ 0 \\ 1 \end{bmatrix}$	$\begin{bmatrix} -0.707 \\ -0.707 \\ 0 \end{bmatrix}$
z_8	$\begin{bmatrix} 0 \\ 1 \\ 0 \end{bmatrix}$	$\begin{bmatrix} 0 \\ 0 \\ 1 \end{bmatrix}$
z_9	$\begin{bmatrix} 0 \\ 0 \\ 1 \end{bmatrix}$	$\begin{bmatrix} 0 \\ 0 \\ 1 \end{bmatrix}$

3.4.3 Discussion of System Zeros

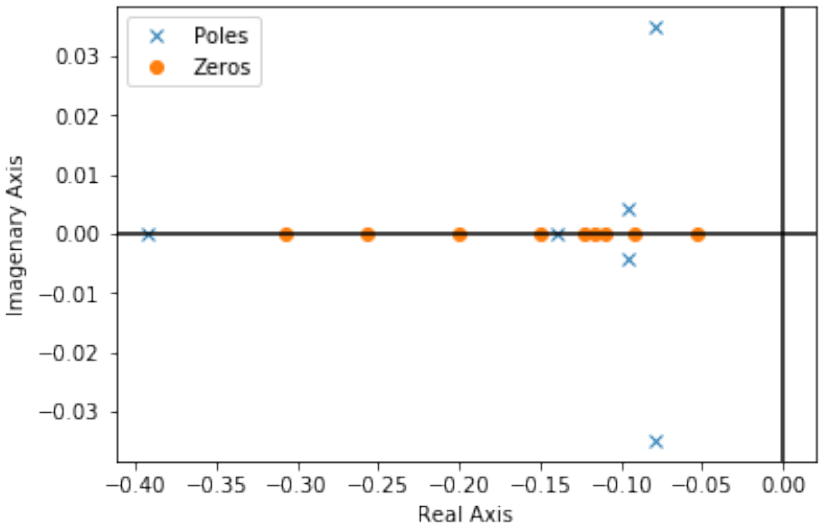

Figure 6: A graphical representation of the system's poles and zeros.

References

Çengel, Y A and Ghajar, A J (2015) *Heat and Mass Transfer*, 5th ed. McGraw-Hill, New York.

Forster, K and Zuber, N (1955) "Dynamics of vapour bubbles and boiling heat-transfer" *AIChE Jl*, *1*, 531.